

# Henry's Law and Synergism in Dilute Near-Critical Solutions: Theory and Simulation

F. Munoz, T. W. Li, and E. H. Chimowitz

Dept. of Chemical Engineering, University of Rochester, Rochester, NY 14627

*An asymptotic analysis based on Taylor series expansions is used for first-order correction terms to the Henry's law approximation to describe solvation phenomena in multiple solute-multiple solvent systems. The magnitude of these correction terms in solvent systems very near their critical points is of particular concern, as shown in model fluid calculations with the aid of integral equation theory. The results clearly demonstrate that close proximity to the critical point in pure and mixed solvent systems causes the Henry's law approximation to show large errors in predicting solubilities, especially near the critical azeotrope of a mixed solvent system. Theoretical results also show that cross solubility enhancements in a two solute-supercritical solvent system cause cooperative synergism (both solute solubilities are increased relative to the corresponding single solute situations) or reverse synergism (both depressed relative to the single solute situation). It appears to be consistent with the available data. In computer simulations, the solute's infinitely dilute reference state is often used as a basis for describing solute thermodynamic behavior. These simulations are best achieved in the canonical ensemble because of the weak composition dependence of free energies in terms of characteristic variables of this ensemble.*

## Introduction

The Henry's law approximation, used widely for describing phase equilibria in dilute solutions, is based on the use of the infinite dilution limit of a solute's chemical potential (or equivalently its fugacity coefficient) extrapolated to predict solution properties at finite concentrations of this species. This approximation is a convenient and often used method for estimating thermodynamic properties in dilute solutions, notwithstanding the assumptions involved in its use. In both theoretical and computer simulation studies in dilute supercritical mixtures, the infinite dilute reference state has often been used to represent solution properties (Shing and Chung, 1987, 1988; Petsche and Debenedetti, 1989; McGuigan and Monson, 1987, 1990; Cochran and Lee, 1988, 1989; Wu et al., 1990; Munoz and Chimowitz, 1992; Li et al., 1993; Tom and Debenedetti, 1993). In simulations the solute's infinite dilution property is usually estimated by using a single solute species in an ensemble of finite size and the resultant solute concentration is thus necessarily finite.

The issue here concerns the accuracy of the Henry's law approach for predicting solution properties, especially for dilute mixtures near their respective critical points. For these and other issues this article uses both a thermodynamic analysis and integral equation theory calculations for the terms that provide the first-order correction to the Henry's law assumption. Calculations for model fluids include both pure and mixed solvent systems near their respective critical point conditions. The theory used is based on the Kirkwood-Buff formalism with the Percus-Yevick closure used for the integral equation calculations. In recent comparisons with simulation results, including those very near the critical point of the system (Li et al., 1993), this theory has proven to be quite accurate and valuable for investigating the thermodynamic properties of dilute supercritical solutions (McGuigan and Monson, 1987, 1990; Cochran and Lee, 1988, 1989; Wu et al., 1990; Munoz and Chimowitz, 1992, 1993a,b; Tom and Debenedetti, 1993). Particularly near the critical point, the Henry's law approxi-

mation is prone to large errors because of the strong synergistic solvation effects that are characteristic of these solutions (Munoz and Chimowitz, 1993a,b).

## Thermodynamic Analysis

At low dilutions *Henry's law* states that the solute fugacity can be found from the following relationship:

$$\hat{f}_1 = x_1 k_1 \quad (1)$$

where  $k_1$  is the solute Henry's law constant defined as:

$$k_1(T, P) \equiv \lim_{x_1 \rightarrow 0} \frac{\hat{f}_1}{x_1} = P \lim_{x_1 \rightarrow 0} \frac{\hat{f}_1}{x_1 P} = P \hat{\phi}_1^\infty \quad (2)$$

where  $\hat{\phi}_1^\infty$  is the fugacity coefficient in the infinite dilution limit and  $P$  is the system pressure. Equation 2 can be used to estimate solubilities of low vapor pressure solutes in dilute supercritical solutions. The standard approach here is to treat the phase equilibrium problem as that of a pure solute in equilibrium with a supercritical solution consisting of itself and solvent molecules (Kurnik and Reid, 1982). In this case the Henry's law prediction of the solute's solubility is given by the result:

$$x_{1H} = \frac{P_1^s}{k_1} = \frac{P_1^s}{P \hat{\phi}_1^\infty} \quad (3)$$

where  $P_1^s$  is the vapor pressure of the solid and the usually quite small Poynting correction has been neglected. Equation 3 can be quite accurate at conditions removed from the critical region of the solvent. However, Eq. 3 can lead to considerable *underestimation* of the solubility in near-critical solvent systems with the magnitude of this error depending on the proximity to the critical point of the solvent. Another problem arising with Eq. 3 is that it predicts that solubilities in systems with two or more solutes present are a superposition of the underlying binary solubilities at the same conditions of temperature and pressure (solute(i)-solvent); it therefore fails to account for synergistic solution effects that are common in these kinds of systems (Chialvo, 1993; Munoz and Chimowitz, 1993a,b) as can be observed in some of the experimental data available in the literature (see the ternary data of Kurnik and Reid, 1982).

## Binary solutions

A systematic way to improve upon Eq. 3 is to expand  $\ln \hat{\phi}_1$  in a Taylor series about the infinite dilution limit and use a suitable truncated form in the expression  $x_1 = P_1^s / P \hat{\phi}_1^y$ , where  $\hat{\phi}_1^y$  is the fugacity coefficient of the solute in the fluid phase. This approach is similar to that adopted in other recent articles analyzing multicomponent solution behavior in supercritical fluids (Jonah and Cochran, 1994; Chialvo, 1993). Here we briefly illustrate the methodology for a dilute solute(1) dissolved in a pure solvent(2). The Taylor series expansions of  $\ln \hat{\phi}_1$  and  $\ln \hat{\phi}_2$  around  $x_1 = 0$  are:

$$\ln \hat{\phi}_1 = \ln \hat{\phi}_1^\infty + \sum_{n=1}^{\infty} \frac{1}{n!} \left( \frac{\partial^n \ln \hat{\phi}_1}{\partial x_1^n} \right)_{T,P}^{(x_1=0)} (x_1)^n \quad (4)$$

$$\ln \hat{\phi}_2 = \ln \hat{\phi}_{2,pure} + \sum_{n=1}^{\infty} \frac{1}{n!} \left( \frac{\partial^n \ln \hat{\phi}_2}{\partial x_1^n} \right)_{T,P}^{(x_1=0)} (x_1)^n \quad (5)$$

Using the Gibbs-Duhem equation (Prausnitz et al., 1986) at constant  $T$  and  $P$  in Eqs. 4 and 5, it is easy to show that the coefficients within the summation sign in Eq. 4 are related to those in Eq. 5. These relationships are:

$$\lim_{x_1 \rightarrow 0} \left( \frac{\partial \ln \hat{\phi}_2}{\partial x_1} \right)_{T,P} = 0 \quad (6)$$

$$\lim_{x_1 \rightarrow 0} \left[ \frac{1}{n!} \left( \frac{\partial^{n+1} \ln \hat{\phi}_2}{\partial x_1^{n+1}} \right)_{T,P} + \frac{1}{(n-1)!} \left( \frac{\partial^n \ln \hat{\phi}_1}{\partial x_1^n} \right)_{T,P} - \frac{1}{(n-1)!} \left( \frac{\partial^n \ln \hat{\phi}_2}{\partial x_1^n} \right)_{T,P} \right] = 0 \quad (7)$$

Using Eqs. 6 and 7 in Eqs. 4 and 5 leads to the following expansions for  $\ln \hat{\phi}_1$  and  $\ln \hat{\phi}_2$  around the infinite dilution condition:

$$\ln \hat{\phi}_1 = \ln \hat{\phi}_1^\infty - K_{11} x_1 + \text{higher-order terms} \quad (8)$$

$$\ln \hat{\phi}_2 = \ln \hat{\phi}_{2,pure} + \frac{1}{2} K_{11} x_1^2 + \text{higher-order terms} \quad (9)$$

where

$$K_{11} = - \left( \frac{\partial \ln \phi_1}{\partial x_1} \right)_{T,P}^\infty \quad (10)$$

These expansions are valid everywhere except at the critical point of the solvent itself where the term  $K_{11}$  diverges. Thus at all other conditions, including the first-order correction terms in the Taylor series for the fugacity coefficients leads to the following equations for  $\hat{\phi}_1$  and  $\hat{\phi}_2$ :

$$\hat{\phi}_1 = \hat{\phi}_1^\infty \exp(-K_{11} x_1) \quad (11)$$

$$\hat{\phi}_2 = \hat{\phi}_{2,pure} \exp\left(\frac{1}{2} K_{11} x_1^2\right) \quad (12)$$

Similar results in a binary system were presented by Debenedetti and Kumar (1986) in their study of infinite dilution fugacity coefficients in binary mixtures.

## Higher-order solutions

We now generalize the previous analysis to a quaternary system consisting of two solutes denoted as components 1 and 2, dissolved in a two component mixed solvent system denoted as components 3 and 4, with a relative composition  $r = x_4/x_3$ . This framework was chosen since it fits the nature of the integral equation calculations we consider in the results section. Setting the parameter  $r$  equal to zero reverts to the case of a pure solvent with two solutes studied experimentally by Kurnik and Reid (1982) while  $x_2$  equal to zero leads to the previously considered case of one solute dissolved in a solvent. We initially

consider expressions for the two solute species and then focus on relationships for the solvent molecules.

The Taylor series expansions of  $\ln \hat{\phi}_1$  and  $\ln \hat{\phi}_2$  as a function of  $x_1$  and  $x_2$  at constant  $T$ ,  $P$ , and  $r = x_4/x_3$  in the limit  $x_1 \rightarrow 0$  and  $x_2 \rightarrow 0$  are given by:

$$\ln \hat{\phi}_1 = \ln \hat{\phi}_1^\infty + \left( \frac{\partial \ln \hat{\phi}_1}{\partial x_1} \right)_{T,P,x_2,r}^\infty x_1 + \left( \frac{\partial \ln \hat{\phi}_1}{\partial x_2} \right)_{T,P,x_1,r}^\infty x_2 + \text{higher-order terms} \quad (13)$$

$$\ln \hat{\phi}_2 = \ln \hat{\phi}_2^\infty + \left( \frac{\partial \ln \hat{\phi}_2}{\partial x_2} \right)_{T,P,x_1,r}^\infty x_2 + \left( \frac{\partial \ln \hat{\phi}_2}{\partial x_1} \right)_{T,P,x_2,r}^\infty x_1 + \text{higher-order terms} \quad (14)$$

where the superscript  $\infty$  denotes the limit  $x_1 \rightarrow 0$ ,  $x_2 \rightarrow 0$ ,  $x_3(1+r) \rightarrow 1$ . We define the parameters  $K_{ij}$  with  $i = 1, 2$ ;  $j = 1, 2$  as:

$$K_{ij} \equiv - \left( \frac{\partial \ln \hat{\phi}_i}{\partial x_j} \right)_{T,P,x_k \neq j,1}^\infty = G_{ij} + F_{ij}; \quad \text{solute-solute derivatives} \quad (15)$$

In the infinite dilution limit where  $x_1 \rightarrow 0$ ,  $x_2 \rightarrow 0$  and  $x_3 + x_4 \rightarrow 1$ , the functions  $G_{ij}$  and  $F_{ij}$  are given by:

$$G_{ij} = \frac{v}{kT} \left[ \left( \frac{\partial P}{\partial x_i} \right)_{T,\rho,x_j,r}^\infty \left( \frac{\partial P}{\partial x_j} \right)_{T,\rho,x_i,r}^\infty \right] K_T \quad (16)$$

$$F_{ij} = \mathcal{C}_{ij} + \sum_{m=3}^4 \sum_{n=3}^4 x_m x_n \mathcal{C}_{mn} - \sum_{m=3}^4 x_m (\mathcal{C}_{im} + \mathcal{C}_{jm}) \quad (17)$$

where the terms  $\mathcal{C}_{ij}$  are integrals of the direct correlation functions  $c_{ij}(r)$ , as shown below (O'Connell, 1971; Chandler, 1987):

$$\mathcal{C}_{ij} \equiv \rho \int c_{ij}(r) dV = - \frac{N}{kT} \left( \frac{\partial \mu_i^r}{\partial N_j} \right)_{T,V,N_k} \quad (18)$$

where  $\mu_i^r = \mu_i(T, V, N_1, N_2) - \mu_i^{IG}(T, V, N_1, N_2)$  is the residual chemical potential, and  $\mu_i^{IG}$  is the ideal gas chemical potential of species  $i$ . The derivation of Eqs. 15–17 is provided in Appendix A where general expressions for a multisolute-multi-solvent system are developed.

Thus, the Taylor series expansions retaining the first-order composition dependent correction terms lead to the following results, analogous to those provided by Jonah and Cochran (1994), for the solute fugacity coefficients in multicomponent solvent systems:

$$\hat{\phi}_1 = \hat{\phi}_1^\infty e^{-K_{11}x_1} e^{-K_{12}x_2} \quad (19)$$

$$\hat{\phi}_2 = \hat{\phi}_2^\infty e^{-K_{22}x_2} e^{-K_{12}x_1} \quad (20)$$

The Taylor expansions for the *solvent fugacity coefficients* in this quaternary system ( $r = x_4/x_3 > 0$ ) are:

$$\ln \hat{\phi}_3 = \ln \hat{\phi}_3^\infty + \left( \frac{\partial \ln \hat{\phi}_3}{\partial x_1} \right)_{T,P,x_2,r}^\infty x_1 + \left( \frac{\partial \ln \hat{\phi}_3}{\partial x_2} \right)_{T,P,x_1,r}^\infty x_2 + \text{higher-order terms} \quad (21)$$

$$\ln \hat{\phi}_4 = \ln \hat{\phi}_4^\infty + \left( \frac{\partial \ln \hat{\phi}_4}{\partial x_1} \right)_{T,P,x_2,r}^\infty x_1 + \left( \frac{\partial \ln \hat{\phi}_4}{\partial x_2} \right)_{T,P,x_1,r}^\infty x_2 + \text{higher-order terms} \quad (22)$$

where the superscript  $o$  denotes the limit  $x_1 \rightarrow 0$  and  $x_2 \rightarrow 0$ , the same limit as denoted by the superscript  $\infty$ . We use the designation  $o$  for properties of the solvent, as in  $\hat{\phi}_3^\infty$  instead of  $\hat{\phi}_3^\infty$  to avoid the erroneous interpretation of it meaning the limit  $x_3 \rightarrow 0$ . Notice that contrary to the case in Eq. 9 for the binary system, the leading composition dependent terms in Eqs. 21 and 22 appear to be linear instead of quadratic. We now attempt to clarify this situation. For the solvents we define the parameters  $K_{ij}$  with  $i = 1, 2$  and  $j = 3, 4$  as:

$$K_{ij} \equiv - \left( \frac{\partial \ln \hat{\phi}_i}{\partial x_j} \right)_{T,P,x_k,r}^\infty = G_{ij} + F_{ij}; \quad \text{solute-solvent derivatives} \quad (23)$$

The functions  $G_{ij}$  in Eq. 23 are given by:

$$G_{i3} = x_4 \frac{v}{kT} \left[ \left( \frac{\partial P}{\partial x_3} \right)_{T,\rho}^\infty \left( \frac{\partial P}{\partial x_i} \right)_{T,\rho,x_j,r}^\infty \right] K_T \quad (24)$$

$$G_{i4} = -x_3 \frac{v}{kT} \left[ \left( \frac{\partial P}{\partial x_3} \right)_{T,\rho}^\infty \left( \frac{\partial P}{\partial x_i} \right)_{T,\rho,x_j,r}^\infty \right] K_T \quad (25)$$

where

$$\left( \frac{\partial P}{\partial x_3} \right)_{T,\rho}^\infty = N \left[ \left( \frac{\partial P}{\partial N_3} \right)_{T,V,N_4}^{N_1=0, N_2=0} - \left( \frac{\partial P}{\partial N_4} \right)_{T,V,N_3}^{N_1=0, N_2=0} \right] \quad (26)$$

and the  $F_{ij}$ s are given by Eq. 17. The derivation of  $G_{ij}$  and  $F_{ij}$  in Eq. 23 is the same as that given in Appendix A with the only difference that the partial molar volumes of components 3 and 4 are given by the expressions:

$$\rho \bar{V}_3^\infty = 1 + x_4 \left( \frac{\partial P}{\partial x_3} \right)_{T,\rho}^\infty K_T \quad (27)$$

$$\rho \bar{V}_4^\infty = 1 - x_3 \left( \frac{\partial P}{\partial x_3} \right)_{T,\rho}^\infty K_T \quad (28)$$

Using the Gibbs-Duhem equation we now show that  $K_{13}$  and  $K_{14}$  are not independent, and the same is true for  $K_{23}$  and  $K_{24}$ . In the limit  $x_1 = x_2 = 0$  the Gibbs-Duhem equation requires that:

$$x_3 \left( \frac{\partial \ln \hat{\phi}_3}{\partial x_1} \right)_{T,P,x_2,r}^\infty + x_4 \left( \frac{\partial \ln \hat{\phi}_4}{\partial x_1} \right)_{T,P,x_2,r}^\infty = 0 \quad (29)$$

$$x_3 \left( \frac{\partial \ln \hat{\phi}_3}{\partial x_2} \right)_{T,P,x_1,r}^o + x_4 \left( \frac{\partial \ln \hat{\phi}_4}{\partial x_2} \right)_{T,P,x_1,r}^o = 0 \quad (30)$$

using Eq. 23 in Eq. 29 and Eq. 30 we have:

$$x_3 K_{13} + x_4 K_{14} = 0 \quad (31)$$

$$x_3 K_{23} + x_4 K_{24} = 0 \quad (32)$$

It is straightforward to verify that Eqs. 23, 24, 25 and 17 satisfy Eqs. 31 and 32.

Using Eqs. 23, 31 and 32 in Eqs. 21 and 22 we find that:

$$\ln \hat{\phi}_3 = \ln \hat{\phi}_3^o + rK_{14}x_1 + rK_{24}x_2 \quad (33)$$

$$\ln \hat{\phi}_4 = \ln \hat{\phi}_4^o - K_{14}x_1 - K_{24}x_2 \quad (34)$$

One immediate difference between this multisolute-multi-solvent case and the binary situation is clear from these equations. While the dependence in Eq. 9 is *quadratic* it is *linear* in Eqs. 33 and 34. There is a second more subtle difference, namely that from Eq. 9 the fugacity coefficient of the solvent in a binary near-critical solution is a monotonic increasing function of the solute mole fraction. This is not the case for more than one solvent since from Eqs. 33 and 34 it is clear that if  $\ln \hat{\phi}_3$  increases with  $x_1$  then  $\ln \hat{\phi}_4$  must decrease and vice versa. The same applies with respect to the mole fraction  $x_2$ . For the sake of completeness an analysis with the Gibbs-Duhem constraints in this multicomponent system is provided in Appendix B.

## Synergistic Effects in Supercritical Solutions

The results from the previous section can be used to interpret the nature of synergistic effects in supercritical solutions. We proceed to analyze some of these cases pointing out the salient results of each situation. For a binary solute-solvent system  $G_{ii}$  for the solute species is strictly positive from Eq. 16. Furthermore, the isothermal compressibility  $K_T \geq 0$  exhibits large values in the solvent's near-critical region. In contrast, the functions  $F_{ij}$  given by Eq. 17 are relatively small in magnitude being dependent upon the direct correlation function integrals given in Eq. 18. Hence, in the near-critical region,  $G_{ii} > F_{ii}$  and Eqs. 15 and 11 together imply that for a single solute dissolved in a near-critical solvent, the Henry's law predictions will always underestimate the real solubility. The significance of the extent of this underprediction is illustrated in a subsequent section dealing with numerical calculations. A second consequence of Eqs. 15–20 involves synergistic effects in near-critical solutions consisting of two solutes dissolved in a supercritical solvent. The synergistic solute effect is characterized by the cross exponential terms  $e^{-K_{12}x_i}$  in Eqs. 19 and 20. For most solid solutes, especially large organic molecules dissolved in a pure supercritical fluid, the terms  $(\partial P/\partial x_i)_{T,P}^\infty$  and  $(\partial P/\partial x_2)_{T,P}^\infty$  are negative in what are often referred to as attractive solutions (Debenedetti and Kumar, 1988). Thus, in a typical case where both derivatives between square brackets in Eq. 16 (with  $i=1$  and  $j=2$ ) have the same sign,  $G_{12}$  is guaranteed to be positive. Furthermore, near the solvent critical point  $G_{12}$  will be dominant with respect to  $F_{12}$  because of the divergent behavior of

$K_T$  (see Eq. 16), resulting in  $K_{12}$  being positive. In this situation all the terms  $K_{11}$ ,  $K_{22}$  and  $K_{12}$  are positive. In this case, Eqs. 19 and 20 imply a *positive feedback synergism* in the system, whereby the presence of component 2 enhances the solubility of component 1 which enhances 2, which enhances 1, and so on. The coupling terms  $e^{-K_{12}x_i}$  in Eqs. 19 and 20 show this synergism formally. Consequently, for attractive solutes dissolved in a near-critical solvent, that is, those where  $(\partial P/\partial x_i)_{T,P}^\infty < 0$ , for  $i=1, 2$ , both component solubilities will be enhanced relative to the respective pure component situation. We refer to this effect in multiple solute systems as *cooperative synergism*. Conversely, if  $(\partial P/\partial x_1)_{T,P}^\infty$  and  $(\partial P/\partial x_2)_{T,P}^\infty$  have opposite signs,  $K_{12}$  is negative and Eqs. 19 and 20 predict *reverse synergism*, whereby both solubilities  $x_1$  and  $x_2$  in the mixture are depressed relative to the dissolution of the respective single solutes at similar thermodynamic conditions. Finally, if both solutes show positive behavior,  $(\partial P/\partial x_1)_{T,P}^\infty > 0$  and  $(\partial P/\partial x_2)_{T,P}^\infty > 0$ , then the synergism is once again cooperative.

Thus Eqs. 19 and 20 predict that either *both* solute solubilities  $x_1$  and  $x_2$  are *enhanced* or *both* of them are *depressed* in near-critical solvents, which is in complete agreement with all the data given by Kurnik and Reid (1982) in a wide variety of systems. These equations also predict that the solubility of the less volatile solute in a cooperative system is enhanced the most by the synergistic effect. This can be seen by considering a case where  $x_2$  is an order of magnitude less than  $x_1$  (such as  $x_1/x_2 \approx 10$ ), similar to the case of the naphthalene(1)-phenanthrene(2) solid mixture dissolved in supercritical carbon dioxide, studied by Kurnik and Reid. With the value of  $x_1$  10 times higher than  $x_2$  the cross-enhancement coefficient  $e^{-K_{12}x_2}$  in Eq. 20 is certainly larger than the cross-enhancement that component 2 will cause, given by the coefficient  $e^{-K_{12}x_2}$  in Eq. 19. The observation that the solubility of the less soluble solid is enhanced the most is also clearly in evidence in the experimental data of Kurnik and Reid. Therefore, Eqs. 19 and 20 appear to predict the salient characteristics of multiple solute synergistic effects in multicomponent near-critical solvent mixtures. In contrast Henry's law is incapable of predicting any form of synergism in these systems. These results are summarized in Table 1.

## First-Order Henry's Law Corrections Near Solvent Critical Point

### Integral equation theory calculations

In the previous section we discussed various qualitative characteristics of Eqs. 19 and 20 in predicting solubilities in near-critical mixtures. In this section we study the magnitude of the correction terms to the Henry's law approximation using integral equation calculations. The solubility of solute component 1 in a two solute system, corrected to first order in composition is given by:

$$\frac{x_1}{x_{1HL}} = e^{K_{11}x_1} e^{K_{12}x_2} \quad (35)$$

where  $x_1$  is the solubility corrected to first order and  $x_{1HL}$  is the Henry's law prediction of its solubility given by Eq. 3. Based on Eq. 35 we define various terms:

$$\text{solute 1, self enhancement} \equiv \exp(K_{11}x_1) \quad (36)$$

**Table 1. Synergistic Effects of Two Solutes in a Supercritical Solvent: Components 1 and 2**

	$\left(\frac{\partial P}{\partial x_1}\right)_{T,\rho}^{\infty}$	$\left(\frac{\partial P}{\partial x_2}\right)_{T,\rho}^{\infty}$	$K_{12}$
Cooperative synergism*	<0	<0	>0
	>0	>0	>0
Reverse synergism**	<0	>0	<0
	>0	<0	<0

\*Cooperative synergism means the solubilities of both solutes in the ternary system are enhanced over their values in their respective binary mixtures at the same solvent conditions.

\*\*Reverse synergism means the solubilities of both solutes in the ternary system are depressed over their values in their respective binary mixtures at the same solvent conditions.

$$\text{solute 1, cross enhancement} \equiv \exp(K_{12}x_2) \quad (37)$$

$$\text{solute 2, cross enhancement} \equiv \exp(K_{12}x_1) \quad (38)$$

Also, the *percentile self enhancement of solute 1* is defined as  $(\exp(K_{11}x_1) - 1) * 100(\%)$ , with similar expressions for the percentile cross enhancements where applicable.

The calculations of the functions in Eqs. 15–18 first require the determination of the direct correlation functions denoted by  $c_{ij}$ s. This was done by solving the Ornstein-Zernike equation for multicomponent systems using the procedure described by Munoz and Chimowitz (1992). After determining the direct correlation functions, the integral quantities given by the  $c_{ij}$ s were calculated with the use of Eq. 18. The derivatives  $(\partial P/\partial x_i)_{T,\rho,x_j,r}^{\infty}$  were then calculated using Eq. A-11 in the Appendix. The isothermal compressibility can be obtained from the result  $K_T = [\rho kT(1 - \sum x_i x_j c_{ij})]^{-1}$ . Expressions for other

**Table 2. Lennard-Jones Parameters: System I**

$\sigma_{11}/\sigma_{22}$	1.661
$\epsilon_{11}/\epsilon_{22}$	2.460
$\kappa_{12}$	0.00

The cross parameters were calculated using Lorentz-Berthelot rules:  $\sigma_{ij} = \frac{1}{2}(\sigma_{ii} + \sigma_{jj})$  and  $\epsilon_{ij} = (1 - \kappa_{ij})(\epsilon_{ii}\epsilon_{jj})^{1/2}$ .

related functions are provided in the Appendix. The pressure when needed was calculated using Baxter's equation (1970).

Figure 1 shows the correction term with respect to the Henry's law prediction for a binary solute(1)-solvent(2) system with the intermolecular parameters of System I shown in Table 2 (Munoz and Chimowitz, 1993b). The temperature is the approximate critical temperature of the solvent ( $T_c^* = kT_c/\epsilon_{22} = 1.32$ ). The self enhancement results are shown at three different levels of the mole fraction  $x_1$ . These calculations show that even very low solubilities can lead to significant underestimation of the solubility close enough to the critical point of the solvent. Figure 2 shows similar calculations at a higher temperature ( $T^* = kT/\epsilon_{22} = 1.35$ ). These calculations show that this effect subsides as we move away from the critical point, consistent with the decrease in  $K_T$  in this region (see Eq. 16). These results suggest that Henry's law provides a reasonable approximation at *very low solubilities* (such as of the order of  $10^{-5}$ ) at conditions *remote from critical*. The violation of either of these conditions is likely to lead to large discrepancies between the Henry's law result and actual data.

The next set of calculations involves a general multisolute-mixed solvent system where the solvent mixture forms a critical azeotrope. Such systems have several interesting features ex-

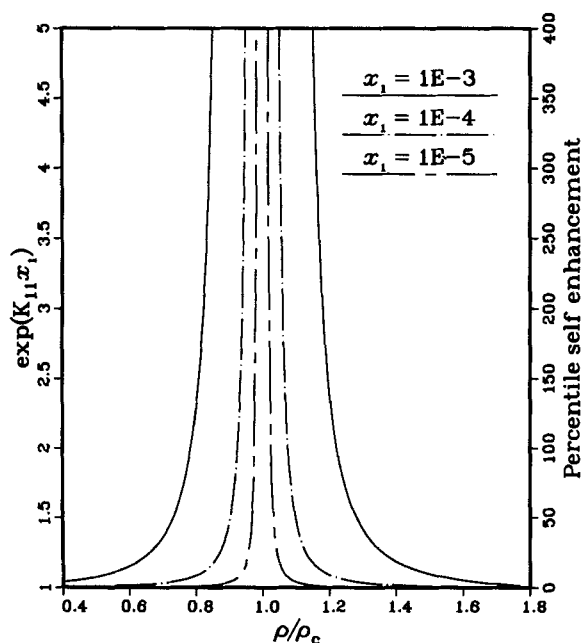


**Figure 1. Self enhancements of the solute(1) dissolved in a pure solvent(2) along the critical isotherm of the solvent ( $T_c^* = 1.32$ ).**

Calculations are shown at various values of the mole fraction of the solute.

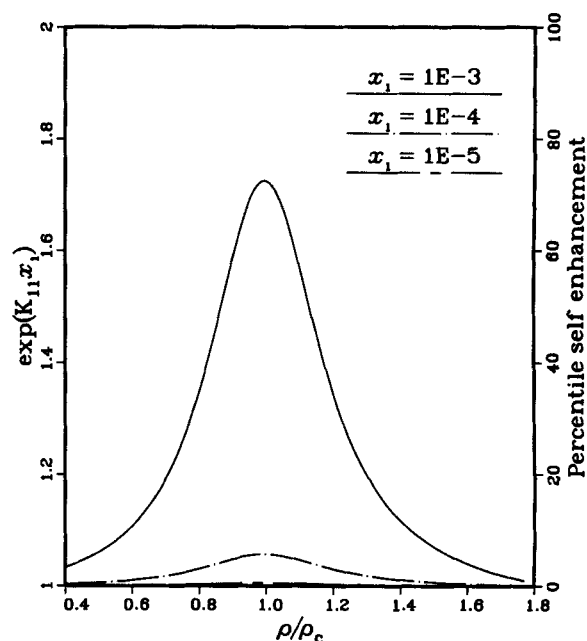


**Figure 2. Self enhancements of the solute(1) dissolved in a pure solvent(2) at a temperature above the critical temperature of the solvent ( $T^* = 1.35 > T_c^*$ ).**

Calculations are shown at various values of the mole fraction of the solute.

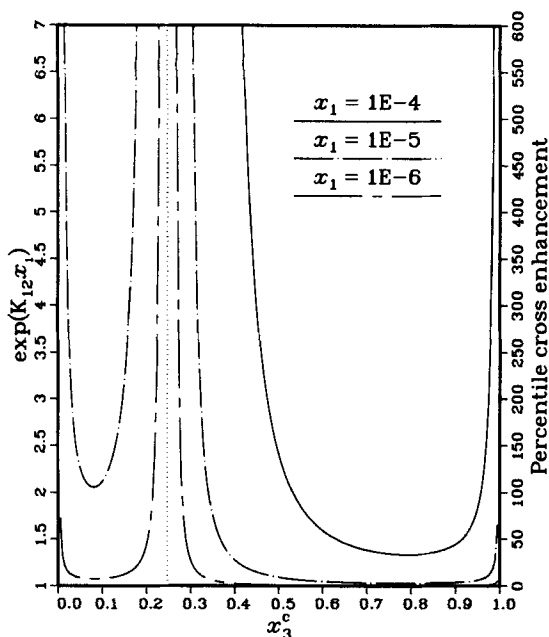


**Figure 3. Synergistic enhancements of component 2 of System II, along the critical line of the solvent mixture at various values of the mole fraction of solute 1.**

hibiting both similarities and differences to the behavior of a dilute mixture near the pure solvent's critical point. A significant difference between these two types of systems is found in the behavior of the isothermal compressibility  $K_T$  along the critical line path. While  $K_T$  diverges as a simple pole along this path for the pure solvent case, it diverges quadratically along the same path for the critical azeotropic mixture as solvent (Munoz and Chimowitz, 1993a,b). This has implications for this analysis of synergism, since  $K_T$  is directly related to synergistic effects through Eqs. 15–20 provided earlier. Figure 3 shows the solute 2 synergistic cross enhancement resulting from the presence of a second solute, component 1 in a critical azeotrope forming mixed solvent system. The Lennard-Jones intermolecular parameters for this system were taken from our previous work and are listed in Table 3. The coordinates of the critical azeotrope are listed in Table 4. The cross enhancements in Figure 3 were calculated along the critical line of the mixed solvent system, which was also obtained from our previous calculations (Munoz and Chimowitz, 1993b). These calculations allow one to compare the cross enhancements near both pure solvent critical points, as well as the critical azeo-

**Table 3. Lennard-Jones Parameters: System II**

$\sigma_{11}/\sigma_{33}$	1.592	$\sigma_{44}/\sigma_{33}$	1.050
$\epsilon_{11}/\epsilon_{33}$	2.026	$\epsilon_{44}/\epsilon_{33}$	0.900
$\sigma_{22}/\sigma_{33}$	1.661	$\epsilon_{34}/\epsilon_{33}$	0.882
$\epsilon_{22}/\epsilon_{33}$	2.460	$\kappa_{34}$	0.07

The cross parameters were calculated using Lorentz-Berthelot rules:

$\sigma_{ij} = \frac{1}{2}(\sigma_{ii} + \sigma_{jj})$  and  $\epsilon_{ij} = (1 - \kappa_{ij})(\epsilon_{ii}\epsilon_{jj})^{1/2}$ ; also  $\kappa_{12} = \kappa_{13} = \kappa_{14} = \kappa_{23} = \kappa_{24} = 0$ ;  $\kappa_{34} \neq 0$ . The solutes are components 1 and 2, while the solvents are components 3 and 4. This system exhibits positive azeotropy, as defined in Rowlinson and Swinton (1982).

**Table 4. Critical Azeotrope Coordinates**

System II		Pure Components	
		$T_c^*$	
$x_3^{az}$	0.248	$T_c^*$	1.320
$P_c^{az}$	0.104	$T_c^*$	1.188
$\rho_c^{az}$	0.252		
$T_c^{az}$	1.186		

Temperature, density and pressure are given on a reduced basis with respect to the solvent component 3. The reduced variables are defined as:  $T^* = kT/\epsilon_{33}$ ,  $\rho^* = N\sigma_{33}^3/V$ ,  $P^* = P\sigma_{33}^3/\epsilon_{33}$ . Thus  $T_c^* = 1.32 * \epsilon_{44}/\epsilon_{33}$ . Note that  $x_1 = x_2 = 0$ ,  $x_3 = x_3^{az}$  and  $x_4 = 1 - x_3^{az}$ .

tropic point, and at critical points removed from both these conditions.

The calculations in Figure 3 illustrate a number of interesting points. Firstly, the synergistic effects around the critical azeotropic condition are much stronger than in the vicinity of the pure solvent critical point at both extremes of the critical line. Even very low solute concentrations (of the order of  $10^{-6}$ ) around the solvent's critical azeotrope exert strong enhancement effects in the system. The Henry's law approximation in this region is likely to show significant error underpredicting solubilities. Along the solvent's critical locus where there is *no azeotrope formation*, solute synergistic effects are much smaller even though the solvent system is at or near its critical point. This implies that under these conditions the Henry's law approximation is likely to be more accurate. Near both pure solvent critical points, solute interactive effects are once again quite significant.

## Computer Simulation in Dilute Solutions: Some Implications

While the calculations of the correction terms in Eqs. 35–38 are in principle straightforward using integral equation theory, a question naturally arises as to how these may be found using the methods of computer simulation. In this part of this article we focus upon issues that are directly related to problems associated with computer simulation in very dilute mixtures. Simulations assume particular importance for systems where more realistic intermolecular potentials (such as the site-site approach) may be used to represent molecular interactions. In such cases, analytic results are much less developed and often not available, hence the need for simulation methods to generate these results. From a theoretical standpoint, the self-enhancement factor  $\exp(K_{11}x_1)$  given in Eq. 36 can be related to various of the system correlation functions using the Kirkwood-Buff theory (1951). This provides that

$$K_{11} = \rho (G_{11} + G_{22} - 2G_{12})^\infty \quad (39)$$

where subscript 1 denotes the solute and subscript 2 denotes the solvent. The  $G_{ij}$  terms are defined by:

$$G_{ij} \equiv \int_V (g_{ij}(r) - 1) dV \quad (40)$$

These properties can in principle be established during the course of the simulations by including an algorithm to calculate the various pair correlation functions  $g_{11}(r)$ ,  $g_{12}(r)$  and  $g_{22}(r)$

**Table 5. Lennard-Jones Potential Parameters\***

	1-1	1-2	2-2
System III			
$(\epsilon_{ij}/k)$ , K	378.76	278.43	204.68
$\sigma_{ij}$ , Å	5.363	4.597	3.831
System IV**			
$(\epsilon_{ij}/k)$ , K	629.49	353.20	204.68
$\sigma_{ij}$ , Å	5.363	4.597	3.831

\*Component 1 is the solute and component 2 is the solvent.

\*\*From Shing and Chung (1987).

and their integrals defined in Eq. 40. The evaluation of  $G_{11}$  in particular poses a special challenge for simulation methods. This is because of the dilemma provided by having to meet the requirement of both extreme dilution, as well as a sufficient number of solute molecules to provide reasonable statistics for the calculation of  $G_{11}$ . As pointed out by Jonah and Cochran (1994), accommodating both requirements simultaneously would appear to require large system sizes for the simulations, at obviously greatly increased computational times. We now present some results of having investigated this issue using complementary insights afforded by both theoretical calculations and simulation results as a guide for answering the question concerning what dilution may reasonably be considered infinitely dilute for the purposes of establishing  $G_{11}$  using the simulation methods.

#### Computer simulation of pair correlation functions in dilute solutions

Calculations in two model Lennard-Jones systems (see Table 5 for the potential parameters), representative of larger solute species dissolved in a smaller solvent fluid, were done in which we investigated the composition dependence of all the solution pair correlation functions over dilution ranges ranging from infinite dilution to up to 2% solute in supercritical solutions. Some quite representative results from these calculations are shown in Figures 4 and 5; they illustrate a very weak com-

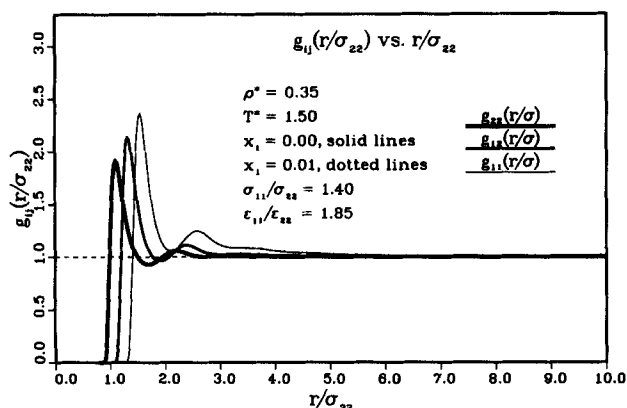


**Figure 4. Radial distribution functions calculated with the Percus-Yevick equation for the Lennard-Jones system III in Table 5, with solute mole fraction  $x_1=0$  and  $x_1=0.01$ .**

The solute is component 1 and the solvent is component 2.

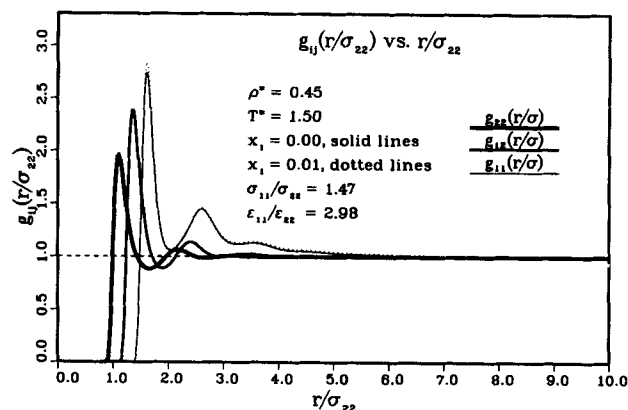


**Figure 5. Radial distribution functions calculated with the Percus-Yevick equation for the Lennard-Jones system IV in Table 5, with solute mole fraction  $x_1=0$  and  $x_1=0.01$ .**

The solute is component 1 and the solvent is component 2.

position dependence in these properties, and in fact for Figure 4 the results for the infinite dilution case and 1% solute are virtually indistinguishable. These results suggested that reasonable system sizes, involving of the order of 10–20 solute species in an ensemble consisting of 1,000 molecules, may provide good simulation statistics for the pair correlation functions, hence the enhancement factor described in Eq. 39. In pursuing this point several simulations were done using the potential parameters of system III in Table 5. The algorithm for these calculations was described in our recent article (Li et al., 1993). The first set of results were developed for 20 solute species in a 1,000 member ensemble using  $5 \times 10^6$  sampling steps. Figure 6 shows a comparison between the integral equation results at the limit of infinite dilution, and the simulations which are necessarily at finite concentration. The spatial domain considered is approximately four molecular diameters, the region primarily responsible for contributions to the solute chemical potential (Munoz and Chimowitz, 1992). There is good agreement between both sets of results except for  $g_{11}(r)$ . In order to improve upon these results for  $g_{11}(r)$  we repeated these calculations and increased the number of sampling steps by an order of magnitude to  $5 \times 10^7$ . A significant improvement resulted, as can be seen from the results presented in Figure 7. We note that the solute composition used here was significantly larger than that used by Chialvo and Debenedetti (1993) who used ten solute species in a 4,000 member ensemble in their molecular dynamics calculations of  $g_{11}(r)$  in a model Lennard-Jones system.

Finally, we comment here on the choice of ensemble type used for simulations in dilute near-critical mixtures. In the literature on this topic there has generally been very little discussion about the preference of one ensemble over another for these sorts of calculations, and in our view this is an important consideration. The use of computer simulation methods with finite sample sizes necessarily implies the use of finite solute concentrations, even when values for an infinite dilution property are sought. For dilute solute systems similar to those considered here, one is confronted with a potential dilemma in the choice of values for the solute mole fraction to use in these simulations. This is compounded by the issue addressed

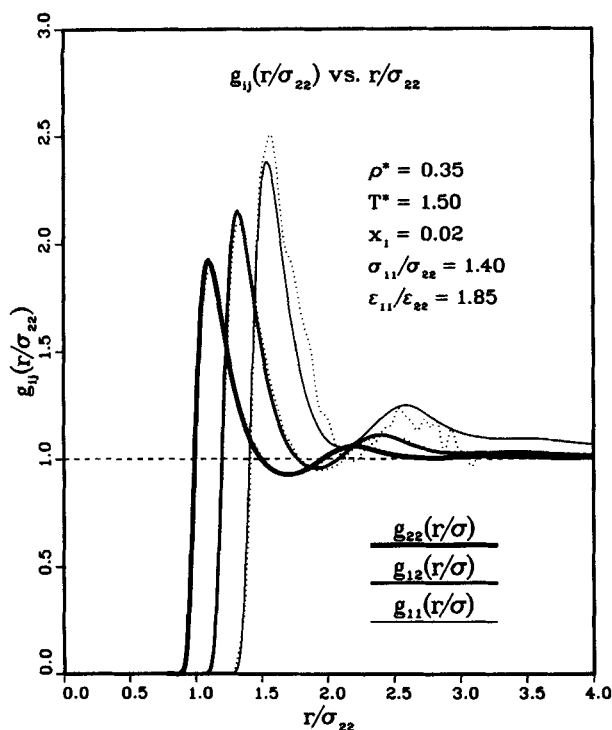


**Figure 6. Radial distribution functions for the Lennard-Jones system III in Table 5, with solute mole fraction  $x_1 = 0.02$ .**

Solid line calculated with the Percus-Yevick equation and dotted lines calculated with Monte Carlo simulations using  $5 \times 10^6$  sampling steps. The solute is component 1 and the solvent is component 2.

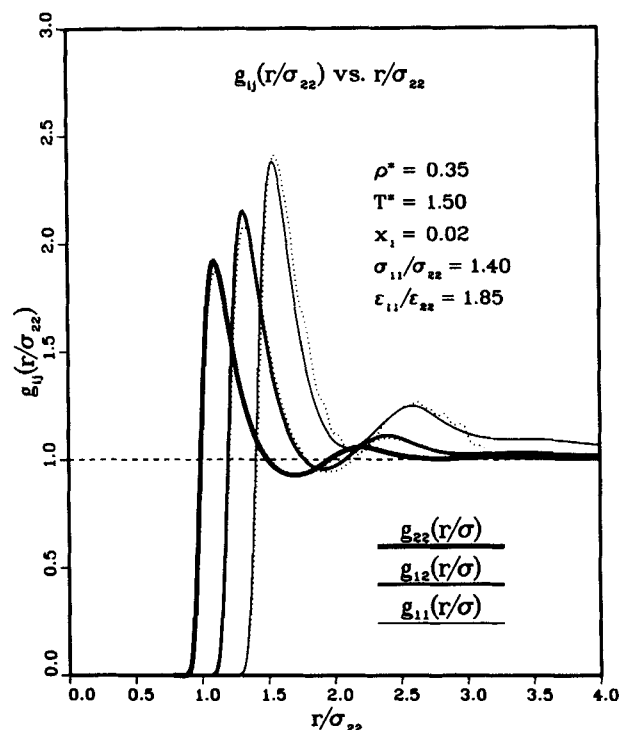


**Figure 7. Radial distribution functions for the Lennard-Jones system III in Table 5, with solute mole fraction  $x_1 = 0.02$ .**

Solid line calculated with the Percus-Yevick equation and dotted lines calculated with Monte Carlo simulations using  $5 \times 10^7$  sampling steps. The solute is component 1 and the solvent is component 2.

previously where solute-solute pair correlations at infinite dilution may be required from the simulations, and for these properties finite solute mole fractions are required for accuracy. While we know from statistical mechanics that all ensembles are equivalent in the thermodynamic limit where the number of particles is extremely large, this equivalence should not be assumed to be the case for finite ensembles of the size typically used in simulations. Hence one is faced with the establishment of a small, finite but as yet unknown solute mole fraction in the ensemble in order to approximate a property at the limit of infinite dilution. *In this case it seems clear that the ensemble with the weakest composition dependence on solute mole fraction in the dilute solute regime should be the ensemble of choice.* Here we show that in near-critical solutions this is the canonical ensemble as opposed to the isothermal-isobaric ensemble which is one that has often been used for these sorts of calculations. The key reason for this result can be seen by comparing the composition dependence of the solute fugacity coefficients along both an isobaric path (corresponding to a NPT ensemble) and an isochoric path (corresponding to a canonical ensemble). The isobaric result has previously been discussed (see Eqs. 13 and 14) while the isochoric case is:

$$\ln \hat{\phi}_1 = \ln \hat{\phi}_1^\infty + \left( \frac{\partial \ln \hat{\phi}_1}{\partial x_1} \right)_{T, \rho, x_2, r}^\infty x_1 + \left( \frac{\partial \ln \hat{\phi}_1}{\partial x_2} \right)_{T, \rho, x_1, r}^\infty x_2 + \text{higher-order terms} \quad (41)$$

$$\ln \hat{\phi}_2 = \ln \hat{\phi}_2^\infty + \left( \frac{\partial \ln \hat{\phi}_2}{\partial x_2} \right)_{T, \rho, x_1, r}^\infty x_2 + \left( \frac{\partial \ln \hat{\phi}_2}{\partial x_1} \right)_{T, \rho, x_2, r}^\infty x_1 + \text{higher-order terms} \quad (42)$$

While the leading terms in Eqs. 13–14 are large and diverge near a critical point (see Eqs. 15 and 16), the corresponding terms in Eqs. 41–42 for the isochoric case are finite and of moderate value, involving simple summations of direct correlation function integrals  $\mathcal{C}_{ij}$  as shown in Eq. A-10 in Appendix A. For the simplest case of a single solute(1) dissolved in a single solvent(2) we have the following expressions for the composition dependence of the solute fugacity coefficient along an isobar and an isochore:

$$\hat{\phi}_1 = \hat{\phi}_1^\infty \exp(-K_{11}x_1); \quad \text{isobaric path} \quad (43)$$

and

$$\hat{\phi}_1 = \hat{\phi}_1^\infty \exp((\mathcal{C}_{12} - \mathcal{C}_{11})x_1); \quad \text{isochoric path} \quad (44)$$

Since in the limit as the critical point of the pure solvent is approached, the quantity  $K_{11}$  diverges this shows that the NPT ensemble will provide a much stronger solute composition dependence in the dilute region than calculations using the canonical ensemble which is thus the preferred ensemble here. We illustrate this point with calculations along both isobaric and isochoric paths. Two representative paths are shown in Figure



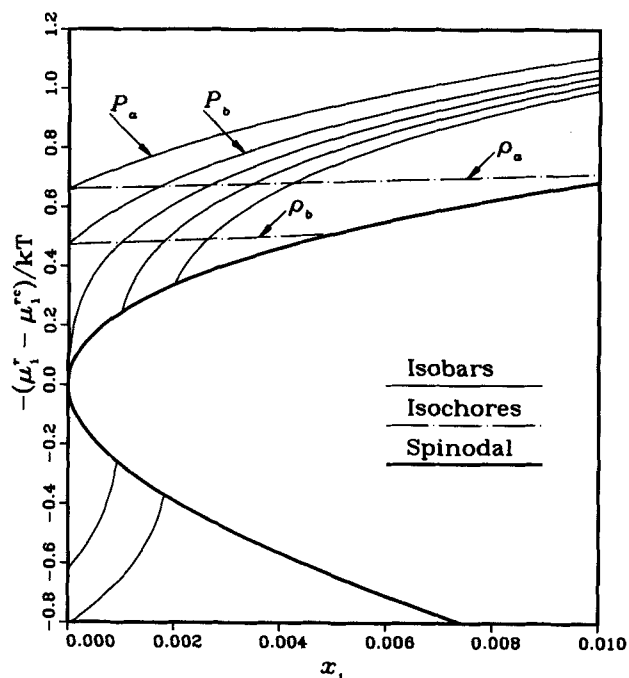


**Figure 8. Chemical potential vs. solute mole fraction.**

Calculated with the Percus-Yevick equation for system III in Table 5, showing alternative paths (isobaric and isochoric) for the calculation of infinite dilution chemical potential.

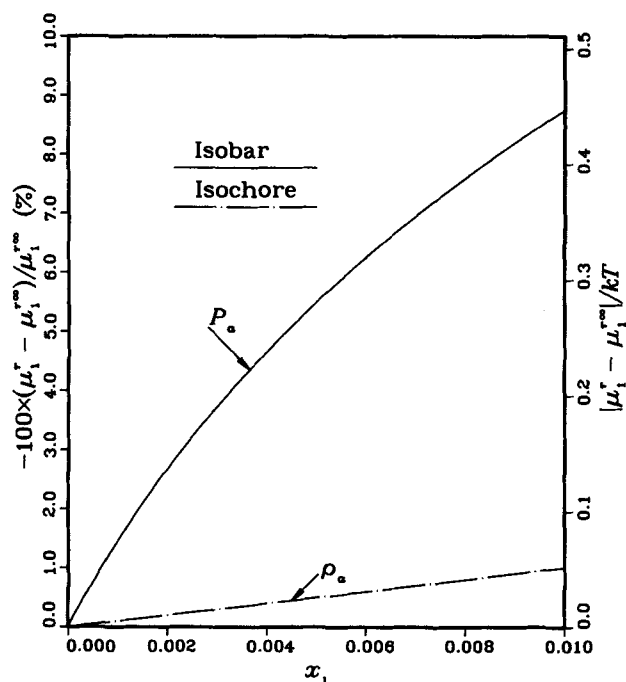


**Figure 9. Deviations of the solute chemical potential with respect to the infinite dilution case vs. mole fraction along an isobaric and an isochoric path.**

The percentile deviation in the fugacity coefficient  $\hat{\phi}_1$  is an exponential function of the deviation in  $\mu_1^r$ , given by  $\Delta\hat{\phi}_1(\%) = [\exp(|\mu_1^r - \mu_1^{r\infty}|/kT) - 1] \times 100$ .

**Table 6. Coordinates of Isobaric and Isochoric Paths**

	Set a	Set b	Crit. Values
$P\sigma_{22}^3/\epsilon_{22}$	0.1316	0.1296	0.1285
$\rho\sigma_{22}^3$	0.3650	0.3401	0.2811
$P/P_c$	1.0240	1.0090	1
$\rho/\rho_c$	1.30	1.21	1

8. In Figure 9 are results for the solute chemical potential calculated at various finite concentrations of the solute along paths symbolized by path *a* in Figure 8. The milder variation in chemical potential with solute concentration along the isochoric path is strikingly evident. In ensembles of the size that have been typically used for supercritical simulations, solute mole fractions of the order 0.2–1.0% have been used for approximating infinite dilution conditions of the solute (such as a single solute particle in a 100–500 member ensemble). The results in Figures 8 and 9 cover this range in both ensembles and clearly point out the advantage of the canonical ensemble. The numerical values of the isobaric and isochoric paths shown in Figure 8 are listed in Table 6. Figure 9 shows a detailed comparison of these paths for set *a*. In Figure 9 at  $x = 0.01$  the isochoric value deviates from  $\mu_1^{r\infty}$  about 1%, while the isobaric value deviates 8.5%. A value of 8.5% might seem acceptable, however, the deviation of the fugacity coefficient  $\hat{\phi}_1(x_1 = 0.01)$  from  $\hat{\phi}_1^{\infty}$  increases exponentially with respect to the deviation in  $\mu_1^r$ , since the deviation in the fugacity coefficient is given by  $\Delta\hat{\phi}_1(\%) = [\exp(|\mu_1^r - \mu_1^{r\infty}|/kT) - 1] \times 100$ . In turn the solubility is proportional to the fugacity coefficient; thus errors in the solubility are of the same magnitude as those of the fugacity coefficient. Using the values in the righthand side of Figure 9 we can find that the deviation of  $\hat{\phi}_1(x_1 = 0.01)$  is ~57% for the isobaric calculation and only 5% for the isochoric calculation. This shows a clear advantage in using the NVT ensemble for these kinds of calculations over the NPT ensemble. In addition the linearity of the isochore of  $\mu_1^r$  with composition means that the slope of the isochore can be calculated in principle by simply performing the simulations at two mole fractions (say  $x_1 = 0.01$  and 0.02). Knowing the slope, it is then straightforward to obtain  $\mu_1^{r\infty}$ . This is not possible in the isobaric case because of the nonlinearity of that function with composition, as shown in Figures 8 and 9.

In summary, these results demonstrate the composition effects on the chemical potential and related properties quite clearly. Therefore, we conclude that in simulations for infinite dilution solute free energies the ensemble that shows the weakest dependence on small, but finite, solute concentrations should preferably be used. In this case one may increase solute numbers modestly (beyond a single particle), thereby promoting improved statistics for  $G_{11}$ , and yet change the value of the property of interest very slightly. For the Henry's constant in near-critical mixtures the results shown here point to the use of the canonical ensemble.

## Conclusions

The analysis in this article has focused upon the investigation of synergistic solvation effects in multisolute–multisolute systems. This first-order analysis provides correction terms to the infinite dilution approximation (more commonly referred to

as Henry's law) using asymptotic expansions. In addition, the magnitude of the various correction terms defined here have been illustrated with calculations done on model fluids using integral equation theory. The results presented have shown that synergistic effects are particularly important near both pure solvent critical points as well as the solvent critical azeotrope in a mixed solvent system where such an azeotrope exists. In both of these situations the Henry's law approximation is likely to show significant error in predicting solute solubilities, often off by a factor of 4 or 5, based on these results. At critical points along the mixed solvent critical line, away from both the critical line extremes as well as the solvent mixture azeotrope, the synergistic effects are markedly smaller. This suggests that in these regions the Henry's law result is more accurate notwithstanding the fact that the solvent system may be near its critical point. Furthermore, general results were presented pertaining to synergistic effects in a two solute-supercritical solvent system. It was shown that in these sorts of systems, solubility enhancements, relative to the single solute situation at the same conditions of temperature and pressure can *either* be positive for both solutes *or* negative for both. The former situation is referred to as cooperative synergism, while the latter is termed reverse synergism. This result is consistent with many of the available experimental data in such systems.

Finally, we discussed the implications of the results of this article for computer simulation methods where the infinite dilution property is the one of interest. In this regard the choice of number of solute particles and ensemble type used is important for calculating the Henry's law correction factors. The results here suggest that the canonical ensemble is particularly suitable for supercritical mixtures and that solute concentrations as high as one mole percent may yield good values for the solute's free energy at the limit of infinite dilution.

## Acknowledgment

The authors would like to acknowledge the National Science Foundation which supported this work through grant No. CBT-9213276.

## Notation

$c_{ij}(r)$  = Ornstein-Zernike direct correlation function  
 $C_{ij} = \rho \int c_{ij}(r) dV = -N/kT(\partial \mu_i^f / \partial N_i)_{T,V,N_k}$   
 $f_i$  = fugacity of component  $i$   
 $F_{ij}$  = contributing term in  $K_{ij}$  (Eq. 17)  
 $g_{ij}(r)$  = molecular pair distribution function  
 $G_{ij}$  = contributing term in  $K_{ij}$  (Eq. 16)  
 $k$  = Boltzmann's constant  
 $K_T = (\partial \ln \rho / \partial P)_{T,x_i}$  = isothermal compressibility  
 $K_{ij} = -(\partial \ln \hat{\phi}_i / \partial x_j)_{T,P,x_k,r} = G_{ij} + F_{ij}$ ; coefficients in Taylor expansion of fugacity coefficient  
 $N$  = number of molecules  
 $P^* = P\sigma^3/\epsilon$  = reduced pressure  
 $r$  = ratio of the mixed solvent mole fraction ( $r = x_4/x_3$ )  
 $r$  = intermolecular distance  
 $r^* = r/\sigma_{22}$  = reduced distance  
 $T^* = kT/\epsilon_{22}$  = reduced temperature  
 $u(r)$  = intermolecular potential  
 $v$  =  $V/N$  = molecular volume  
 $V$  = volume  
 $x_i$  = mole fraction

## Greek letters

$\beta = 1/kT$

$\epsilon$  = Lennard-Jones parameter  
 $\kappa_{12}$  = parameter to account for deviations from Berthelot geometric mean  
 $\mu_i$  = chemical potential  
 $\mu_i^f = \mu_i(T, V, N_i, N_2) - \mu_i^{IG}(T, V, N_i, N_2)$  = solute residual chemical potential  
 $\rho$  =  $N/V$  = number density  
 $\rho^* = N\sigma_{22}^3/V$  = reduced density  
 $\sigma$  = Lennard-Jones parameter  
 $\hat{\phi}_i$  = fugacity coefficient of component  $i$  ( $= f_i/x_i P$ )

## Subscripts

$i$  = component  $i$   
 $az$  = property at azeotropic point  
 $c$  = property at a critical state

## Superscripts

$r$  = residual property  
 $*$  = reduced property  
 $x_i = 1$  = property at limit  $x_i \rightarrow 1$   
 $x_i = 0$  = property at limit  $x_i \rightarrow 0$   
 $c$  = property at a critical state  
 $az$  = property at azeotropic point  
 $-$  = partial molar property  
 $\infty$  = property at infinite dilution  
 $IG$  = ideal gas state

## Literature Cited

- Baxter, R. J., "Ornstein-Zernike Relation and Percus-Yevick Approximation for Fluid Mixtures," *J. Chem. Phys.*, **52**, 4559 (1970).  
Chandler, D., *Introduction to Modern Statistical Mechanics*, Oxford University Press, New York (1978).  
Chialvo, A. A., "Solute-Solute and Solute-Solvent Correlations in Dilute Near-Critical Ternary Mixtures: Mixed-Solute and Entrainer Effects," *J. Phys. Chem.*, **97**, 2740 (1993).  
Chialvo, A. A., and P. G. Debenedetti, "Molecular Dynamics Study of Solute-Solute Microstructure in Attractive and Repulsive Supercritical Mixtures," *Ind. Eng. Chem. Res.*, **31**, 1391 (1992).  
Cochran, H. D., and L. L. Lee, "General Behavior of Dilute Binary Solutions," *AIChE J.*, **34**, 170 (1988).  
Cochran, H. D., and L. L. Lee, "Solvation Structure in Supercritical Fluid Mixtures Based on Molecular Distribution Functions," *Supercritical Fluid Science and Technology*, K. P. Johnston and J. M. L. Penninger, eds., ACS Symp. Ser., 406 (1989).  
Debenedetti, P. G., and S. K. Kumar, "Infinite Dilution Fugacity Coefficients and the General Behavior of Dilute Binary Systems," *AIChE J.*, **32**, 1253 (1986).  
Debenedetti, P. G., and S. K. Kumar, "The Molecular Basis of Temperature Effects in Supercritical Extraction," *AIChE J.*, **34**, 645 (1988).  
Jonah, D., and H. D. Cochran, "Chemical Potentials in Dilute, Multicomponent Solutions," *Fluid Phase Equilib.*, **92**, 107 (1994).  
Kurnik, R. T., and R. C. Reid, "Solubility of Solid Mixtures in Supercritical Fluids," *Fluid Phase Equilib.*, **8**, 93 (1982).  
Li, T. W., F. Munoz, and E. H. Chimowitz, "Computer Simulation and Theory for Free Energies in Dilute Near-Critical Solutions," *AIChE J.*, **39**, 1985 (1993).  
McGuigan, D. B., and P. A. Monson, "Vapour-Liquid Critical Lines Predicted by Distribution Function Theories," *Molec. Phys.*, **62**(1), 3 (1987).  
McGuigan, D. B., and P. A. Monson, "Analysis of Infinite Dilution Partial Molar Volumes Using a Distribution Function Theory," *Fluid Phase Equilib.*, **57**, 227 (1990).  
Munoz, F., and E. H. Chimowitz, "Integral Equation Calculations of the Solute Chemical Potential in a Near-Critical Fluid Environment," *Fluid Phase Equilib.*, **71**, 237 (1992).  
Munoz, F., and E. H. Chimowitz, "Critical Phenomena in Mixtures: I. Thermodynamic Theory for the Binary Critical Azeotrope," *J. Chem. Phys.*, **99**, 5438 (1993a).

- Munoz, F., and E. H. Chimowitz, "Critical Phenomena in Mixtures: II. Synergistic and Other Effects Near Mixture Critical Points," *J. Chem. Phys.*, **99**, 5450 (1993b).
- O'Connell, J. P., "Thermodynamic Properties of Solutions Based on Correlation Functions," *Molec. Phys.*, **20**, 27 (1971).
- Petsche, I. B., and P. G. Debenedetti, "Solute-Solvent Interactions in Infinitely Diluted Supercritical Mixtures: A Molecular Dynamics Investigation," *J. Chem. Phys.*, **91**, 7075 (1989).
- Prausnitz, J. M., R. N. Lichtenthaler, and E. G. Azevedo, *Molecular Thermodynamics of Fluid-Phase Equilibria*, Prentice-Hall, Englewood Cliffs, NJ (1986).
- Rowlinson, J. S., and F. L. Swinton, *Liquids and Liquid Mixtures*, Butterworth Scientific, London (1982).
- Shing, K. S., and S. T. Chung, "Computer Simulation Methods for the Calculation of Solubility in Supercritical Extraction Systems," *J. Phys. Chem.*, **91**, 1674 (1987).
- Shing, K. S., and S. T. Chung, "Calculation of Infinite-Dilution Partial Molar Properties by Computer Simulation," *AIChE J.*, **34**, 1973 (1988).
- Tom, J. W., and P. G. Debenedetti, "Integral Equation Study of Microstructure and Solvation in Model Attractive and Repulsive Supercritical Mixtures," *Ind. Eng. Chem. Res.*, **32**, 2118 (1993).
- Wu, R., L. L. Lee, and H. D. Cochran, "Structure of Dilute Supercritical Solutions: Clustering of Solvent and Solute Molecules and the Thermodynamic Effects," *Ind. Eng. Chem. Res.*, **29**, 977 (1990).

## Appendix A

Analytic expressions are developed for the first-order corrections to the Henry's law for a multisolute-multisolute system. There are a total of  $c$  components, composed by  $\nu$  solutes and  $c-\nu$  solvents. The  $c-\nu$  solvents remain at a constant relative composition. To indicate this we use the parameters  $r_j$ , such that:

$$x_j = x_{\nu+1} r_j; \quad j = \nu+2, \dots, c \quad (\text{A1})$$

We are looking to determine analytic expressions for the parameters:

$$K_{ij} \equiv - \left( \frac{\partial \ln \phi_i}{\partial x_j} \right)_{T, P, x[j], \mathcal{L}}^\infty \quad (\text{A2})$$

where the notation  $x[j]$  indicates that  $x_1, x_2, \dots, x_{j-1}, x_{j+1}, \dots, x_\nu$  remain constant, and  $r$  indicates that the ratios  $r_{\nu+2}, \dots, r_c$  remain constant also. The following thermodynamic identity allow us to work in terms of the residual chemical potential:

$$\begin{aligned} \left( \frac{\partial \ln \hat{\phi}_i}{\partial x_j} \right)_{T, P, x[j], \mathcal{L}}^\infty &= \frac{1}{kT} \left( \frac{\partial \mu_i}{\partial x_j} \right)_{T, P, x[j], \mathcal{L}}^\infty - \frac{\delta_{ij}}{x_i} \\ &= \frac{1}{kT} \left( \frac{\partial \mu_i}{\partial x_j} \right)_{T, P, x[j], \mathcal{L}}^\infty \end{aligned} \quad (\text{A3})$$

Since  $\bar{V}_i = (\partial \mu_i / \partial P)_{T, x_1, \dots, x_c}$  then it is straightforward to show that:

$$\left( \frac{\partial \mu_i}{\partial x_j} \right)_{T, P, x[j], \mathcal{L}}^\infty = \left( \frac{\partial \mu_i}{\partial x_j} \right)_{T, P, x[j], \mathcal{L}}^\infty + \bar{V}_i \left( \frac{\partial P}{\partial x_j} \right)_{T, P, x[j], \mathcal{L}}^\infty \quad (\text{A4})$$

The derivatives of the residual chemical potential are related to those of the total chemical potential by the equations:

$$\frac{1}{kT} \left( \frac{\partial \mu_i}{\partial x_j} \right)_{T, P, x[j], \mathcal{L}}^\infty = \frac{1}{kT} \left( \frac{\partial \mu_i}{\partial x_j} \right)_{T, P, x[j], \mathcal{L}}^\infty - \frac{\delta_{ij}}{x_j} \quad (\text{A5})$$

$$\frac{1}{kT} \left( \frac{\partial \mu_i}{\partial x_j} \right)_{T, P, x[j], \mathcal{L}}^\infty = \frac{1}{kT} \left( \frac{\partial \mu_i}{\partial x_j} \right)_{T, P, x[j], \mathcal{L}}^\infty - \frac{\delta_{ij}}{x_j} \quad (\text{A6})$$

Using Eqs. A5 and A6 in Eq. A4 and taking the infinite dilution limit  $x_1 \rightarrow 0, x_2 \rightarrow 0, \dots, x_\nu \rightarrow 0$  and  $\sum_{j=\nu+1}^c x_j \rightarrow 1$ , we have:

$$\left( \frac{\partial \mu_i}{\partial x_j} \right)_{T, P, x[j], \mathcal{L}}^\infty = \left( \frac{\partial \mu_i}{\partial x_j} \right)_{T, P, x[j], \mathcal{L}}^\infty - \bar{V}_i \left( \frac{\partial P}{\partial x_j} \right)_{T, P, x[j], \mathcal{L}}^\infty \quad (\text{A7})$$

Moreover,

$$\left( \frac{\partial \mu_i}{\partial x_j} \right)_{T, P, x[j], \mathcal{L}}^\infty = N \sum_{m=1}^c \left( \frac{\partial \mu_i}{\partial N_m} \right)_{T, P, N_k}^\infty \left( \frac{\partial N_m}{\partial x_j} \right)_{N[j], N, \mathcal{L}}^\infty \quad (\text{A8})$$

with

$$\left( \frac{\partial N_m}{\partial x_j} \right)_{N[j], N, \mathcal{L}}^\infty = \begin{cases} 1, & \text{for } m=j; \\ 0, & \text{for } m \neq j \text{ and } m \leq \nu; \\ -x_m, & \text{for } m \neq j \text{ and } m > \nu. \end{cases} \quad (\text{A9})$$

Using Eqs. A8 and A9 and Eq. 18 in the main text we obtain

$$\frac{1}{kT} \left( \frac{\partial \mu_i}{\partial x_j} \right)_{T, P, x[j], \mathcal{L}}^\infty = -\mathcal{C}_{ij} + \sum_{m=\nu+1}^c x_m \mathcal{C}_{im} \quad (\text{A10})$$

In an analogous way we arrive at

$$\begin{aligned} \frac{v}{kT} \left( \frac{\partial P}{\partial x_j} \right)_{T, P, x[j], \mathcal{L}}^\infty &= - \sum_{m=\nu+1}^c x_m \mathcal{C}_{jm} \\ &+ \sum_{m=\nu+1}^c \sum_{n=\nu+1}^c x_m x_n \mathcal{C}_{mn} \end{aligned} \quad (\text{A11})$$

For the partial molar volume at infinite dilution we have:

$$\rho \bar{V}_i^\infty = 1 + \left( \frac{\partial P}{\partial x_i} \right)_{T, P, x[i], \mathcal{L}}^\infty K_T \quad (\text{A12})$$

Using Eqs. A10, A11 and A12 in Eq. A7 and also invoking Eqs. A2 and A3 we arrive at:

$$K_{ij} = G_{ij} + F_{ij} \quad (\text{A13})$$

with

$$G_{ij} = \frac{v}{kT} \left[ \left( \frac{\partial P}{\partial x_i} \right)_{T, P, x[j], \mathcal{L}}^\infty \left( \frac{\partial P}{\partial x_j} \right)_{T, P, x[i], \mathcal{L}}^\infty \right] K_T \quad (\text{A14})$$

$$F_{ij} = \mathcal{C}_{ij} + \sum_{m=\nu+1}^c \sum_{n=\nu+1}^c x_m x_n \mathcal{C}_{mn} - \sum_{m=\nu+1}^c x_m (\mathcal{C}_{im} + \mathcal{C}_{jm}) \quad (\text{A15})$$

Replacing  $\nu=2$  and  $c=4$  in Eq. A15 we obtain Eq. 17 in the main text. In a multisolute-multisolvent system the fugacity coefficients corrected to first-order are:

$$\hat{\phi}_i = \hat{\phi}_i^\infty \prod_{j=1}^{\nu} e^{-K_{ij}x_j}; \quad i=1, \dots, \nu \quad (\text{A16})$$

## Appendix B

The Taylor series expansion for the four components fugacity coefficients are given by:

$$\ln \hat{\phi}_k = \sum_{n=0}^{\infty} \sum_{m=0}^{\infty} \frac{x_1^n x_2^m}{n!m!} f_k(n, m) \quad (\text{B1})$$

where  $k=1, 2$  denotes the solutes and  $k=3, 4$  denotes the solvents. The expression  $f_k(n, m)$  is an abbreviation for the partial derivatives:

$$f_k(n, m) = \lim_{\substack{x_1 \rightarrow 0 \\ x_2 \rightarrow 0}} \left( \frac{\partial^{n+m} \ln \hat{\phi}_k}{\partial x_1^n \partial x_2^m} \right)_{T, P, r} \quad (\text{B2})$$

The first term in the series expansion is:

$$f_k(0, 0) = \lim_{\substack{x_1 \rightarrow 0 \\ x_2 \rightarrow 0}} \ln \hat{\phi}_k \quad (\text{B3})$$

The Gibbs-Duhem equation at constant  $T$  and  $P$  for the four component system is:

$$x_1 \ln \hat{\phi}_1 + x_2 \ln \hat{\phi}_2 + x_3 \ln \hat{\phi}_3 + x_4 \ln \hat{\phi}_4 = 0 \quad (\text{B4})$$

Since we have two independent variables  $x_1$  and  $x_2$  then using Eq. B4 we arrive at the following equations:

$$\sum_{k=1}^4 x_k \left( \frac{\partial \ln \hat{\phi}_k}{\partial x_1} \right)_{T, P, x_2, r} = 0 \quad (\text{B5})$$

$$\sum_{k=1}^4 x_k \left( \frac{\partial \ln \hat{\phi}_k}{\partial x_2} \right)_{T, P, x_1, r} = 0 \quad (\text{B6})$$

The mole fractions  $x_3$  and  $x_4$  are dependent variables given by:

$$x_3 = \frac{1 - x_1 - x_2}{1 + r}; \quad x_4 = \frac{r(1 - x_1 - x_2)}{1 + r} \quad (\text{B7})$$

where  $r$  is the ratio  $x_4/x_3$ . Using Eq. B1 we have:

$$\left( \frac{\partial \ln \hat{\phi}_k}{\partial x_1} \right)_{T, P, r} = \sum_{n=0}^{\infty} \sum_{m=0}^{\infty} \frac{x_1^n x_2^m}{n!m!} f_k(n+1, m) \quad (\text{B8})$$

$$\left( \frac{\partial \ln \hat{\phi}_k}{\partial x_2} \right)_{T, P, r} = \sum_{n=0}^{\infty} \sum_{m=0}^{\infty} \frac{x_1^n x_2^m}{n!m!} f_k(n, m+1) \quad (\text{B9})$$

Notice that while the expansions are taken at the limit  $x_1 \rightarrow 0$  and  $x_2 \rightarrow 0$ , we will be considering finite compositions in Eqs. B5–B9. Using Eqs. B7–B9 in Eq. B5 and Eq. B6 we have:

$$\sum_{n=0}^{\infty} \sum_{m=0}^{\infty} \frac{x_1^n x_2^m}{n!m!} [x_1 u_1(n+1, m) + x_2 u_2(n+1, m) + \omega(n+1, m)] = 0 \quad (\text{B10})$$

$$\sum_{n=0}^{\infty} \sum_{m=0}^{\infty} \frac{x_1^n x_2^m}{n!m!} [x_1 u_1(n, m+1) + x_2 u_2(n, m+1) + \omega(n, m+1)] = 0 \quad (\text{B11})$$

where

$$u_1(n, m) = f_1(n, m) - \omega(n, m) \quad (\text{B12})$$

$$u_2(n, m) = f_2(n, m) - \omega(n, m) \quad (\text{B13})$$

$$\omega(n, m) = \frac{1}{1+r} f_3(n, m) + \frac{r}{1+r} f_4(n, m) \quad (\text{B14})$$

The next step is to rearrange Eqs. B10 and B11 by collecting the coefficients of the same power of  $x_1$  and  $x_2$ . Then the coefficients so obtained must equal zero for the series to vanish at arbitrary values of  $x_1$  and  $x_2$ . Setting those terms to zero leads to the Gibbs-Duhem constraints to the coefficients  $f_k(n, m)$  for the quaternary system. These are given below:

$$\omega(1, 0) = \omega(0, 1) = 0 \quad (\text{B15})$$

$$\left[ \frac{u_1(n, 0)}{(n-1)!} + \frac{\omega(n+1, 0)}{n!} \right] = \left[ \frac{u_2(0, n)}{(n-1)!} + \frac{\omega(0, n+1)}{n!} \right] = 0; \quad n=1, \dots, \infty \quad (\text{B16})$$

$$\left[ \frac{u_1(n-1, 1)}{(n-1)!} + \frac{\omega(n, 1)}{n!} \right] = \left[ \frac{u_2(1, n-1)}{(n-1)!} + \frac{\omega(1, n)}{n!} \right] = 0; \quad n=1, \dots, \infty \quad (\text{B17})$$

$$\left[ \frac{u_1(n, m)}{(n-1)!m!} + \frac{u_2(n+1, m-1)}{n!(m-1)!} + \frac{\omega(n+1, m)}{n!m!} \right] = 0; \quad n, m=1, \dots, \infty \quad (\text{B18})$$

$$\left[ \frac{u_1(n-1, m+1)}{(n-1)!m!} + \frac{u_2(n, m)}{n!(m-1)!} + \frac{\omega(n, m+1)}{n!m!} \right] = 0; \quad n, m=1, \dots, \infty \quad (\text{B19})$$

Equations B15–B19 are the analogues to Eqs. 6 and 7 in the main text for the binary system. Notice that Eq. B15 is the same statement as the one made in Eqs. 29 and 30 in the main text.

*Special Case,  $r=0$ .* When  $r=0$  the fourth component is not present and Eq. 34 is no longer needed. Also the linear terms in Eq. 33 vanish; therefore, we need to include the second derivatives of  $\ln \hat{\phi}_3$  in that expansion. Thus for  $r=0$  we have:

$$\ln \hat{\phi}_3 = \ln \hat{\phi}_{3,\text{pure}} + \frac{1}{2} \left( \frac{\partial^2 \ln \hat{\phi}_3}{\partial x_1^2} \right)_{T,P,x_2}^o + \left( \frac{\partial^2 \ln \hat{\phi}_3}{\partial x_1 \partial x_2} \right)_{T,P}^o x_1 x_2 + \frac{1}{2} \left( \frac{\partial^2 \ln \hat{\phi}_3}{\partial x_2^2} \right)_{T,P}^o x_2^2 + \text{higher-order terms} \quad (\text{B20})$$

Using  $n=1$  in Eq. B16, then applying Eq. B15 and setting  $x_4=0$  we arrive at:

$$\left( \frac{\partial^2 \ln \hat{\phi}_3}{\partial x_1^2} \right)_{T,P,x_2}^o = - \left( \frac{\partial \ln \hat{\phi}_1}{\partial x_1} \right)_{T,P,x_2}^\infty = K_{11} \quad (\text{B21})$$

$$\left( \frac{\partial^2 \ln \hat{\phi}_3}{\partial x_2^2} \right)_{T,P,x_1}^o = - \left( \frac{\partial \ln \hat{\phi}_1}{\partial x_2} \right)_{T,P,x_1}^\infty = K_{22} \quad (\text{B22})$$

Also using  $n=1$  in Eq. B17, then applying Eq. B15 and setting  $x_4=0$  we arrive at:

$$\left( \frac{\partial^2 \ln \hat{\phi}_3}{\partial x_1 \partial x_2} \right)_{T,P}^o = - \left( \frac{\partial \ln \hat{\phi}_1}{\partial x_2} \right)_{T,P,x_1}^\infty = - \left( \frac{\partial \ln \hat{\phi}_2}{\partial x_1} \right)_{T,P,x_2}^\infty = K_{12} = K_{21} \quad (\text{B23})$$

Using Eqs. B21–B23 in Eq. B20 we arrive at:

$$\ln \hat{\phi}_3 = \ln \hat{\phi}_{3,\text{pure}} + \frac{1}{2} K_{11} x_1^2 + K_{12} x_1 x_2 + \frac{1}{2} K_{22} x_2^2 + \text{higher-order terms} \quad (\text{B24})$$

Thus when there is only one solvent the first composition dependent term in the solvent's fugacity coefficient is quadratic. This is not the case however when the solvent consists of a mixture of two (or more) components as discussed in detail earlier. The extension of Eq. B24 for a multisolute system of  $\nu$  solutes dissolved in a *single* solvent is:

$$\ln \hat{\phi}_{\nu+1} = \ln \hat{\phi}_{\nu+1}^{\text{pure}} + \frac{1}{2} \sum_{i=1}^{\nu} \sum_{j=1}^{\nu} K_{ij} x_i x_j + \text{higher-order terms} \quad (\text{B25})$$

Equation B25 is a complete analogue to Eq. 9 in the main text.

*Manuscript received Aug. 19, 1993, and revision received March 2, 1994.*